Reactions Induced in Ni⁵⁸ with 0–24 MeV Deuterons: Statistical Model Analysis*

Marshall Blann and George Merkel

Department of Chemistry, University of Rochester, Rochester, New York

(Received 13 March 1963)

Excitation functions for Ni⁵⁸(d,α), $(d,\alpha p)$, $(d,\alpha n)$, $(d,2pn)$, $(d,2np)$, and Ni⁶⁰$(d,2\alpha)$ reactions have been measured radiochemically for deuteron energies up to 24 MeV. The decrease in the (d,α) excitation curve above the threshold of competing reactions such as $(d,\alpha p)$ and $(d,\alpha n)$ is consistent with the qualitative behavior of compound-nucleus reactions. The experimental results have been compared with statistical-model calculations that assume nuclear level densities of the form $\rho(E) \propto (2J+1)E^{-2} \exp[2(aE)^{1/2}]$, where the excitation energy E was corrected for pairing. The value of the parameter a was set equal to the experimental value determined by Brady and Sherr (from alpha-particle energy spectra produced by bombarding Ni⁵⁸ with 15.6- and 19.4-MeV protons). Cross sections were calculated for all permutations of n, p, d, t, He³, and α emission for two successive evaporations, followed by a calculation of a third evaporation of a neutron, proton, or alpha particle where it was energetically possible. In these calculations the inverse cross sections of particles with energy ϵ, $\sigma_{inv}(\epsilon)$, were assumed to be of the following forms: for neutrons, $\sigma_{inv}(\epsilon) = \sigma_1(1+\epsilon_n/\epsilon)$; for charged particles, $\sigma_{inv}(\epsilon) = \sigma_2(1-\epsilon_c/\epsilon)$ when $\epsilon > \epsilon_c$, and $\sigma_{inv}(\epsilon) = 0$ when $\epsilon < \epsilon_c$. The parameters σ_1, ϵ_n, σ_2, and ϵ_c were chosen so that values of $\sigma_{inv}(\epsilon)$ would approximate optical-model calculations of the capture cross sections. Two sets of compound-nucleus excitation functions were calculated. In the first set the alpha-particle and the proton inverse cross sections, $\sigma_{inv}(\epsilon)$, were chosen to correspond to optical-model reaction cross sections calculated with parameters deduced from experimental elastic scattering. In the second set of compound-nucleus excitation function calculations the inverse cross sections, $\sigma_{inv}(\epsilon)$, were chosen to correspond to nuclear radii 10% smaller than those used in the first set of calculations. The experimental excitation functions nearly all fall between the two sets of calculated functions.

I. INTRODUCTION

MANY recent investigations have been oriented toward determining the mechanism of inelastic nuclear reactions at tens of MeV bombarding energies.[1–5] Attempts have been made to determine the extent to which the compound-nucleus mechanism is or is not valid in explaining features of these nuclear reactions. These investigations have included measurement of (a) the energy spectra of emitted particles, (b) angular distributions of emitted particles, (c) recoil range measurements to determine momentum imparted to the struck nucleus, and (d) excitation functions. Attempts are made to show that the spectral shapes and angular distributions of the emitted particles are consistent with those predicted by a statistical-model calculation, that the struck nucleus has received a full momentum transfer from the incident projectile, or that the excitation functions for various reactions have the magnitude, position, and shape predicted by a statistical-model calculation. In the case of excitation functions parameters have often been varied freely in order to obtain agreement between theory and experiment.

In the work described here we have bombarded natural nickel with 0 to 24 MeV deuterons and measured the excitation function for the Ni⁵⁸(d,α)Co⁵⁶, Ni⁵⁸$(d,\alpha n)$Co⁵⁵, Ni⁵⁸$(d,\alpha p)$Fe⁵⁵, Ni⁵⁸$(d,2pn)$Co⁵⁷, Ni⁵⁸$(d,2np)$Ni⁵⁷, and Ni⁶⁰$(d,2\alpha)$Mn⁵⁴ reactions. We then compare the experimental results with theoretical calculations of the compound-nucleus cross sections, where we have attempted as far as possible to use independently determined parameters.

These excitation function measurements and calculations were motivated by the thought that compound-nucleus reactions coupled with compound-nucleus theory as applied to the continuum can be used to study the behavior of highly excited nuclei.

II. EXPERIMENTAL PROCEDURES

A. Targets and Bombardments

Target foils were individually weighed natural nickel foils 21.9 mg/cm² ($\pm 1\%$) thick. Chemical analysis indicated 0.72% cobalt and spectroscopic analysis showed 0.05% iron and 0.07% manganese.[6] Targets consisted of stacks of 30 foils, 1 in. in diameter; the target foil stacks provided more than enough thickness to degrade the 24 MeV deuteron beam to 0 MeV. The bombardments utilized the 24-MeV external deuteron beam of the former University of California 60-in. cyclotron. The target holder served as a Faraday cup. In all, there were four bombardments; integrated beam varied between 0.93 and 2.28 μA-h. The first bombardment was used to determine cross sections for the production of nickel and cobalt isotopes, the second and fourth for iron isotopes, and the third for iron and manganese isotopes.

During the 4-month period in which the bombardments were carried out the deuteron beam energy was measured three times by determining the range of the

* This work supported by the U. S. Atomic Energy Commission and Research Corporation.

[1] See list given by D. Bodansky, R. K. Cole, W. G. Cross, C. R. Gruhn, and I. Halpern, Phys. Rev. **126**, 1082 (1962).

[2] B. G. Harvey, Ann. Rev. Nuc. Sci. **10**, 235 (1960).

[3] L. Winsberg and J. M. Alexander, Phys. Rev. **121**, 518 (1961).

[4] J. M. Alexander and L. Winsberg, Phys. Rev. **121**, 529 (1961).

[5] J. B. J. Read, I. Ladenbauer-Bellis, and R. Wolfgang, Phys. Rev. **127**, 1722 (1962).

[6] We are indebted to D. Sisson and Dr. G. Shalimoff for the analyses.

beam in Al. The measured ranges were 467.3 mg/cm², 464.1 mg/cm², and 468.3 mg/cm². The average of the measured ranges corresponds to 24.0 MeV and the spread in range measurements corresponds to ±0.1 MeV. The range-energy curves of Sternheimer were used to calculate incident deuteron energy as well as deuteron energy versus target thickness in the nickel foils.[7]

B. Chemistry

All targets were dissolved in dilute nitric acid to which appropriate carriers had been added. The final precipitates were covered with 0.1-mil-thick Pliofilm (0.45 mg/cm² rubber hydrochloride).

Co-Ni Separation

The nitrates of cobalt and nickel were converted to chlorides by successive evaporations with $12M$ HCl. The chlorides were adjusted to $8M$ HCl and put through Dowex A-1 anion exchange columns. The cobalt was adsorbed on the column and the nickel eluted. The nickel samples were electroplated on platinum disks. The cobalt samples were eluted with $4M$ HCl and precipitated as $K_3Co(NO_2)_6$.

Co-Ni-Fe-Mn Separation

The samples were dissolved in dilute nitric acid and carriers added. The solution was made basic with NH_4OH and NaOH and the $Fe(OH)_3$ and $Mn(OH)_2$ precipitates were separated from the amino complexes of cobalt and nickel. The hydroxide precipitates were then boiled in conc. NH_4OH, centrifuged and redissolved in fuming HNO_3. $KClO_3$ was added to precipitate MnO_2. This separated the iron from the manganese. To each fraction additional cobalt carrier was added and precipitated as $K_3Co(NO_2)_6$. Additional manganese carrier was added to the iron fraction and additional iron carrier to the manganese fraction and the separations repeated. Finally, manganese was precipitated as MnO_2 and iron was precipitated as the 8-hydroxyquinolate. Gamma spectrum analysis indicated that both the iron and manganese were radiochemically pure.

C. Disintegration Rate Determination

The radiation detected for each isotope observed is listed in Table I.

Calibrated end-window proportional counters were used for all measurements of β^+ radiation. Calibrated NaI crystals ($1\frac{1}{2}$ in.×1 in. and 3 in.×3 in.) were used for γ-ray measurement.[8] The x-ray radiation from Fe⁵⁵ was measured inside a 2-in.-diam proportional counter which was filled with 90% argon-10% methane at 1 atm. The pulses resulting from the Fe⁵⁵ x rays in argon

TABLE I. Radiation types and energies observed for isotopes studied in this work, with abundances used to calculate absolute disintegration rate.

Nuclide	Type of radiation observed	Energy of radiation observed (MeV)	Assumed abundance[a]
Ni⁵⁷	γ	1.39	0.86
	γ	1.89	0.14
	γ	0.120 (Co⁵⁷ daughter)	1.00
Co⁵⁵	β⁺		0.60
Co⁵⁶	γ	1.26+higher energy	[a,b]
Co⁵⁷	γ	0.120	1.00
Fe⁵⁵	K-x ray	0.0059	0.28[c]
Mn⁵⁴	γ	0.84	1.00

[a] D. Strominger, J. M. Hollander, and G. T. Seaborg, Rev. Mod. Phys. 30, 585 (1958).
[b] The radiation from a pure sample of Co⁵⁶ was measured in a 4π proportional counter; a β⁺ abundance of 20% was assumed. The gamma spectrum was then measured with a 3-in.×3-in. NaI crystal and 100-channel pulse-height analyzer. An efficiency was determined for all radiation above 1.26 MeV at a given geometry. This 3-in.×3-in. counter with 1.26-MeV discriminator setting was then used to determine the disintegration rate of all samples. The 1.26-MeV discriminator setting was chosen to avoid erroneous contributions from Co⁵⁸ γ rays.
[c] C. D. Broyles, D. A. Thomas, and S. K. Haynes, Phys. Rev. 89, 715 (1953).

were analyzed with a 512-channel pulse-height analyzer. A geometric factor of 0.5, and a counter efficiency of 0.85 were calculated, and self-absorption corrections were applied to each sample. Because of the large number of corrections for the Fe⁵⁵ disintegration rate we estimate the uncertainty in the cross-section determinations for Fe⁵⁵ to be ±30%. For all other isotopes the uncertainty is estimated to be ±15%. The experimental cross sections are given in Table II.

III. EVAPORATION CALCULATIONS

A. Qualitative Discussion of Experimental Results

The experimental results (Table II) are shown in Figs. 1 and 5 to 10. The competitive behavior of the (d,α) versus the $(d,\alpha n)$, $(d,\alpha p)$, and $(d,2\alpha)$ excitation functions (Fig. 1) is in qualitative agreement with the expected behavior of compound nucleus reactions.[9,10] Angular distribution experiments also indicate that the compound-nucleus reaction mechanism probably makes a large contribution to these excitation functions.[11] The qualitative agreement with compound-nucleus theory can be corroborated in a quantitative manner with a statistical theory calculation.

B. General Discussion

The excitation function calculations in this paper are based on the statistical theory of nuclear reactions in its standard form.[9,12–14] That is, the distribution of nuclear

[7] R. M. Sternheimer, Phys. Rev. 115, 137 (1959).
[8] M. Blann, Phys. Rev. 123, 1356 (1961).

[9] V. F. Weisskopf, Phys. Rev. 52, 295 (1937).
[10] S. N. Ghoshal, Phys. Rev. 80, 939 (1950).
[11] G. Merkel, University of California Lawrence Radiation Laboratory Report UCRL-9898, 1962 (unpublished).
[12] L. Wolfenstein, Phys. Rev. 82, 690 (1951).
[13] T. Ericson and V. Strutinski, Nucl. Phys. 8, 284 (1958).
[14] A. M. Lane and R. G. Thomas, Rev. Mod. Phys. 30, 257 (1958).

TABLE II. Experimental cross sections versus incident deuteron energy.

Incident deuteron energy[a] (MeV)	Cross section (mb) for production of:						
	Ni57	Co57	Co56	Co55	Fe55	Mn54 [b]	Mn54
24.0	42	469	21	46	73	8.3	3.2
23.5	38	435	22	47	73	6.2	2.4
22.9	c	c	c	c	65	4.0	1.5
22.4	29	336	21	46	73	4.0	1.6
21.8	21	289	24	45	77	2.2	0.85
21.4	17	269	25	44	71	1.7	0.66
20.8	14	223	29	46	74	1.4	0.54
20.3	13	184	30	41	66	1.3	0.50
19.6	10.0	128	33	40	67	1.1	0.42
19.0	8.5	115	32	35	48	0.58	0.23
18.3	7.5	68	30	27	48	0.38	0.15
17.7	7.1	69	37	28			
17.0	5.8	62	42	25	21		
16.4	5.0	55	46	21			
15.6	4.1	21	45	14	22		
14.8	c	26	64	14			
14.2	c	14	73	9.0	15		
13.4	1.7	16	81	4.7			
12.6	1.0	8.2	92	1.2	5		
11.7	0.51	4.0	91	0.59			
10.9	0.16		89	0.22	0.7		
9.7	0.10	4.2	71	0.11			
8.8	0.094		37	0.08			
7.5	0.097	1.2	30	0.03			
6.3	0.088		13	0.02			
4.9	0.084	1.7		0.02			
3.5	0.079			0.02			
d	0.085	1.5		0.02			
d	0.076						
d	0.075	0.82					

a The energy loss in each foil can be obtained from the difference between successive incident deuteron energies.
b The cross sections listed for Mn54 in column 7 are calculated as Ni60$(d,2\alpha)$Mn54 reactions; the cross sections in column 8 are calculated as Ni58$(d,\alpha2p)$Mn54 reactions. We cannot distinguish between contributions from the two reactions with data obtained using natural nickel targets.
c Sample lost or contaminated.
d At this depth of target foil stack the deuteron beam has been degraded far below the Ni60 Coulomb barrier. Therefore, the activity in these foils probably results from neutron-induced reactions.

levels in the residual nuclei are assumed to be described by a distribution function of the form

$$\rho(E',J) = (2J+1)\rho(E'), \tag{1}$$

where E' is the excitation energy of the residual nucleus and where J is the angular momentum of the residual nucleus. In rigorous descriptions of the compound-nucleus theory as applied to the continuum, the $(2J+1)$ assumption about the distribution of nuclear levels in the residual nuclei is shown to result in a greatly simplified theory for compound nucleus cross sections.[14,15] In this simplified theory the dependence of nuclear level densities on angular momentum does not explicitly appear in the final expression for the probability of particle emission[9]:

$$P_i(E^*,\epsilon)d\epsilon = \gamma_i \sigma_{\text{inv}}\epsilon \frac{\rho(E')}{\rho(E^*)} d\epsilon, \tag{2}$$

[15] G. R. Satchler, in Proceedings of the Conference on Reactions Between Complex Nuclei, Gatlinburg [Oak Ridge National Laboratory Report ORNL-2606, 1958 (unpublished)], p. 79.

where $P_i(E^*,\epsilon)d\epsilon$ represents the probability per unit time that a nucleus excited to E^* will emit the particle i with channel energy between ϵ and $\epsilon+d\epsilon$; $\gamma_i = g_i m_i/(\pi^2\hbar^3)$, where g_i is the number of spin states of particle i, and m_i is the reduced mass of particle i. The expression $\rho(E')/\rho(E^*)$ is the ratio of the energy level density of the residual nucleus at excitation E' to the energy level density of the initial nucleus at excitation E^*. The inverse cross section σ_{inv} is the cross section for the capture of particle i with kinetic energy ϵ by the residual nucleus at excitation E' to form the initial nucleus with excitation energy E^*.

In these calculations we assume that the level density distributions in nuclei excited to energy E are of the form[16-18]

$$\rho(E) = CE^{-2} \exp[2(aE)^{1/2}]. \tag{3}$$

The value of the parameter C is assumed to be constant; odd-even effects on the nuclear level density are taken into consideration by replacing the excitation energy E by $E-\delta$, where δ represents a displacement in the ground-state energy[19]:

$$\rho(E) = C(E-\delta)^{-2} \exp[2\{a(E-\delta)\}^{1/2}]. \tag{4}$$

Before Eqs. (2) and (4) are used for excitation function calculations values of σ_{inv}, a, and δ must be selected. The validity of calculations based on Eqs. (2) and (4) is dependent upon the accuracy with which these parameters can be determined. An attempt has been made to select the best independently determined experimental values for these parameters.
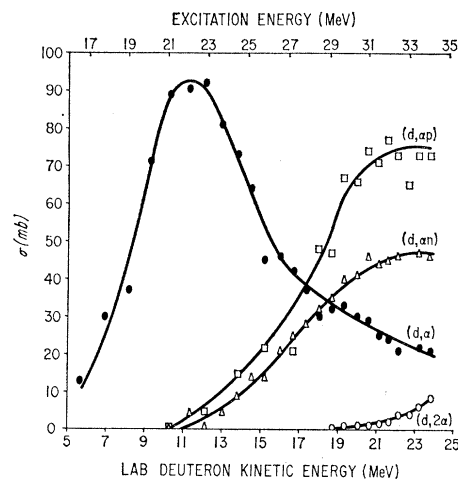
EXCITATION ENERGY (MeV)
17 19 21 23 25 27 29 31 33 35

σ(mb)

(d,αp)
(d,αn)
(d,α)
(d,2α)

LAB DEUTERON KINETIC ENERGY (MeV)

FIG. 1. Experimentally determined excitation functions for the Ni58(d,α)Co56, Ni58$(d,\alpha n)$Co55, Ni58$(d,\alpha p)$Fe55, and Ni60$(d,2\alpha)$Mn54 reactions.

[16] H. A. Bethe, Rev. Mod. Phys. 9, 69 (1937).
[17] T. Ericson, in Proceedings of the International Conference on Nuclear Structure, Kingston, Canada, 1960, edited by D. A. Bromley and E. Vogt (University of Toronto Press, Toronto, 1960), p. 697.
[18] D. W. Lang, Nucl. Phys. 26, 434 (1961).
[19] H. Hurwitz and H. Bethe, Phys. Rev. 81, 898 (1951).

C. Parameters

1. Level Density Parameters

The value of a used in Eq. (4) is 7 MeV^{-1}; this value was determined by Brady and Sherr from analysis of the alpha particle spectra produced by bombarding Ni⁵⁸ with 15.6- and 19.4-MeV protons.[20] Their determination is also based on the tacit assumption that nuclear angular momentum distributions are proportional to $(2J+1)$.

We have taken δ literally to be a pairing energy. The value used was obtained from a plot of $M-A$ versus Z for fixed A in the $A=60$ region; therefore, $\delta=0$ MeV for odd-odd nuclides, $\delta=1.4$ MeV for odd-even nuclides, and $\delta=2.8$ MeV for even-even nuclides.[21]

2. Inverse Cross Sections

Unfortunately, accurate values of the inverse cross sections, σ_{inv}, are not available. Blatt and Weisskopf calculated values of σ_{inv} by assuming a square-well nuclear potential and a purely ingoing nondamped wave inside the nucleus.[22] Values of σ_{inv} can also be obtained with the optical-model nuclear reaction theory. In calculations using the optical-model theory, the optical-model reaction cross section is assumed to be equal to the compound-nucleus inverse cross section. Actually, optical-model reaction cross sections consist of the sum of all inelastic cross sections plus compound elastic cross sections, and not all inelastic reactions result in the formation of a compound nucleus. Another difficulty arises because the available experimentally determined optical-model parameters apply only to target nuclei in their ground state. The inverse cross section nearly always corresponds to the formation of a compound nucleus by the collision of a bombarding particle with a highly excited target nucleus. The variation of the optical-model parameters as a function of bombarding particle energy and target excitation is not accurately known. Ericson has suggested that the Pauli exclusion principle would become less important as target nucleus excitation increased and consequently nuclear transparency would tend to decrease.[23] If the target nucleus absorption density corresponds to a nucleus which is relatively opaque but not metallically shiny, the optical-model reaction cross section might be expected to approach the compound nucleus formation cross section.

The neutron optical-model parameters obtained from analysis of elastic neutron scattering correspond to a fairly transparent nucleus (Fig. 2, curves 2 and 3).[24,25]

[20] F. P. Brady and R. Sherr, Phys. Rev. 124, 1928 (1961).
[21] F. Everling, L. A. Konig, J. H. E. Mattauch, and A. H. Wapstra, Nucl. Phys. 18, 529 (1960).
[22] J. Blatt and V. F. Weisskopf, Theoretical Nuclear Physics (John Wiley & Sons, Inc., New York, 1952).
[23] T. Ericson, in Advances in Physics, edited by N. F. Mott (Taylor and Francis, Ltd., London, 1960), Vol. 9, p. 425.
[24] F. E. Bjorklund and S. Fernbach, in Proceedings of the Second United Nations International Conference on The Peaceful Uses of
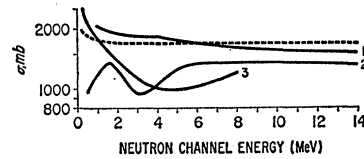
FIG. 2. Capture cross sections for the neutron plus Co⁵⁸ and Cu⁵⁹ reactions. The dashed line is calculated with Eq. (5). Curves 1, 2, and 3 are optical-model calculations. Parameters used are given in Table III. Curves 1 and 2 are for neutrons on Cu⁵⁹; curve 1 has been calculated with an imaginary potential depth of 20 MeV while curve 2 has been calculated using the values suggested in the literature. Curve 3 has been calculated for Co⁵⁸ using an imaginary potential depth of 3 MeV.

Therefore, in our statistical-theory calculations we used optical-model cross sections calculated with a deeper imaginary potential than the value determined from elastic scattering by Bjorklund and Fernbach.[24] The deepening of the imaginary potential yields optical-model reaction cross sections which are similar to the predictions of Blatt and Weisskopf's continuum theory. The optical-model parameters used to calculate the inverse cross sections are given in Table III. The results of these calculations for neutrons, protons, and alpha particles are shown in Figs. 2–4. A deepening of the Gaussian surface absorption potential beyond the values given in Table III had very little effect on the proton or alpha particle optical-model reaction cross sections.

In our compound-nucleus cross-section calculations the probability of He³ and H³ emissions must be calculated. In order to obtain estimates of the He³ and H³ inverse cross sections, optical-model reaction cross sections were obtained using the parameters given in Table III. No attempt is made to justify these parameters, other than the statements that the nuclear radius factor is the same as that used for alpha particles and that the values of σ_{inv} calculated with the optical model are not very sensitive to the values of the real and imaginary potential as long as the imaginary potential is not so small that the nucleus becomes transparent or so large that the nucleus becomes metallically shiny. Machine time restrictions did not permit the calculation of all the necessary inverse cross-section values with an optical-model program. Therefore, optical-model cross sections were approximated with expressions of the following form[26]:

for neutrons,

$$\sigma_{inv}=\sigma_1(1+\epsilon_n/\epsilon); \qquad (5)$$

for charged particles,

$$\sigma_{inv}=\sigma_2(1-\epsilon_c/\epsilon) \quad \text{when} \quad \epsilon>\epsilon_c$$

and

$$\sigma_{inv}=0 \qquad \text{when} \quad \epsilon<\epsilon_c. \qquad (6)$$

Atomic Energy, Geneva, 1958 (United Nations, Geneva, 1958), Vol. 14, p. 24.
[25] E. J. Campbell, H. Feshbach, C. E. Porter, V. F. Weisskopf, MIT Laboratory for Nuclear Science Technical Report No. 73, 1960 (unpublished).
[26] I. Dostrovsky, Z. Fraenkel, and G. Freidlander, Phys. Rev. 116, 683 (1960).

TABLE III. Summary of optical-model parameters used in calculating capture cross sections presented in Figs. 2–4.

Incident particle	Target nucleus	Radius parameter (F)	Projectile size (F)	Diffuseness parameter (F)	Real potential depth (MeV)	Imaginary potential depth (MeV)	Type of absorption	Reference to source of parameters and general details not listed in table
n	Co⁵⁸	1.15	0.40	0.52	52	3	Gaussian surface	a
	Cu⁵⁹	1.25	0	not constant—see Ref.			Gaussian surface	b
	Cu⁵⁹	1.25	0	see Ref.	52	20	Gaussian surface	b
p	Ni⁵⁹	1.25	0	not constant—see Ref.			Gaussian surface	b
α	Co⁵⁶	1.14	2.24	0.50	49.3	11	volume	b
α	Co⁵⁵	1.17	1.77	0.576	50	10.17	volume	c
d	Ni⁵⁸	1.50	0	not constant—see Ref.			volume	d
t	Ni⁵⁷	1.14	2.24	0.50	50	20	volume	b
He³		1.14	2.24	0.50	50	20	volume	b

[a] E. J. Campbell, H. Feshbach, C. E. Porter, and V. F. Weisskopf, MIT Laboratory for Nuclear Science Technical Report No. 73, 1960 (unpublished).
[b] F. E. Bjorklund and S. Fernbach, in *Proceedings of the Second United Nations International Conference on the Peaceful Uses of Atomic Energy, Geneva, 1958* (United Nations, Geneva, 1958), Vol. 14, p. 24. A real spin-orbit depth of 33 MeV was used in these calculations. For charged particles, a square-well charge distribution was used.
[c] J. R. Huizenga and G. J. Igo, Argonne National Laboratory Report No. 6373, 1961 (unpublished).
[d] M. A. Melkanoff, T. Sawada, and N. Andro, Phys. Letters **2**, 98 (1962).

For a specific charged particle the parameter ϵ_c is assumed to vary as

$$\epsilon_c = \epsilon_0 V_i = \epsilon_0 \frac{z_1 z_2 e^2}{r_0 A^{1/3} + \rho}, \qquad (6a)$$

where z_1 is the charge of the emitted particle, z_2 is the charge of the residual nucleus, e is the electron charge, A is the mass number of the residual nucleus, and r_0 and ρ vary according to the charged particle. The parameters of Eqs. (5) and (6) were selected so that cross sections calculated with these equations are in close agreement with optical-model calculations. The values used for these parameters are listed in Table IV. In Figs. 2–4 inverse cross sections for emission of neutrons, protons, and alpha particles calculated with Eqs. (5) and (6) are compared with cross sections calculated using optical-model theory. As shown in these figures, agreement is within 10% or better. After integrating Eq. (2) over all possible particle emission energies, the net discrepancy between values calculated with Eqs. (5) and (6) and optical-model cross sections is found to be less than 5%.

As previously discussed, all inelastic nuclear reactions do not result in compound nucleus formation. Therefore, the optical-model reaction cross sections tend to be larger than the compound-nucleus formation cross section. With this overestimation of compound-nucleus cross sections in mind, we have made a second set of compound-nucleus cross-section calculations. In this second set, the alpha particle and the proton inverse cross sections are calculated with reduced nuclear radii. All other optical-model parameters are kept the same. We cannot justify this reduction in radius other than in terms of the final comparison between experimental excitation functions and calculated excitation functions. Because of the relatively large wavelength of slow neutrons, and because of the absence of Coulomb effects, a 10% reduction in the nuclear radius has relatively small effect on the neutron inverse cross sections. Table IV also gives the values of the parameters used in Eqs. (5) and (6) for the second set of calculations.

3. Compound Nucleus Formation Cross Section

The assumptions made about the deuteron plus Ni⁵⁸ cross sections for compound nucleus formation are very important because calculated emission probabilities are normalized to these values. The loosely bound deuteron has a relatively large probability of undergoing inelastic surface interactions which do not lead to compound nucleus formation. Consequently, for deuteron reactions, the assumption that the optical-model reaction cross section is equal to the compound-nucleus formation cross section can be very inaccurate. Melkanoff has obtained deuteron optical-model parameters by interpreting experimental deuteron elastic scattering data.[27] These parameters yield optical-model reaction cross
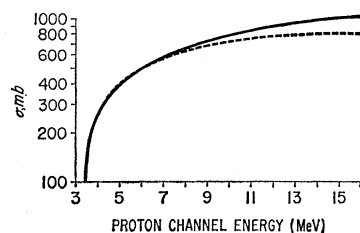

FIG. 3. Capture cross sections for the neutron plus Co⁵⁸ and Cu⁵⁹ reactions. The dashed line is calculated with Eq. (6). The solid line is from an optical-model calculation.

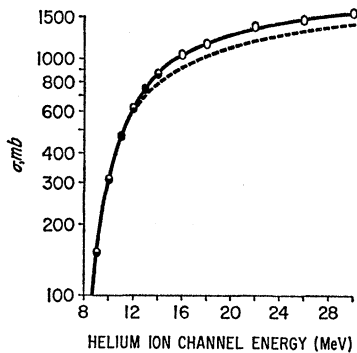[27] M. A. Melkanoff, T. Sawada, and N. Andro, Phys. Letters **2**, 98 (1962).

FIG. 4. Capture cross sections for the alpha particle plus Co⁵⁶ reaction. The dashed line is calculated with Eq. (6). The solid line, filled points, half-filled points, and open points are from optical-model calculations. Parameters are given in Table III. The solid points represent values calculated by Igo and Huizenga; the open points represent values calculated with the Bjorklund-Fernbach program. Half-open and half-closed points represent an overlap of the two sets of calculations.

sections which probably over estimate the compound-nucleus formation cross section. In order to obtain a crude semiclassical approximation to the compound-nucleus formation cross section for the deuteron plus Ni⁵⁸ reaction we have calculated optical-model reaction cross sections using Melkanoff's parameters, but with the radius factor reduced to 1.10 F. We make no attempt to justify this reduction in radius, other than the final comparison between experimental results and our statistical-theory calculation.

D. Computer Program

Equation (2) was integrated on a IBM 7090 computer. The output gave the emission probabilities for 6 different single particle emissions, for 36 different combinations of two particle emission, and the spectra of the excitation energies of residual nuclei after one or two particles had been emitted. The program input consisted of the excitation energy of the compound nucleus,

TABLE IV. Parameters used in Eqs. (4)-(6) to to approximate optical-model cross sections.

Incident particle	σ_c (b)	Parameters of Eqs. (4)-(6)			
		ϵ_n (MeV)	ϵ_0 (MeV)	R_0 (F)	ρ (F)
		First parameter set			
n	1.68	0.048			
p	1.00		0.522	1.70	0
d	1.86		0.814	1.70	1.20
t	1.57		0.640	1.70	1.20
He³	1.86		0.750	1.70	1.20
	1.86		0.814	1.70	1.20
		Second parameter set			
n	1.68	0.048			
p	2.10		0.522	1.50	0
d	1.30		0.814	1.50	1.20
t	1.27		0.640	1.50	1.20
He³	1.33		0.750	1.50	1.20
a	1.33		0.814	1.50	1.20

the binding energies for all emitted particles,[21] and the parameters in Eqs. (5) and (6) that correspond to these particle emissions. The calculation then proceeded as follows:

(1) The first particle to be emitted was chosen (a neutron) and the probabilities for its emission were calculated for all possible kinetic energies beginning at 0.25 MeV (increasing at 0.5-MeV intervals) such that the residual nucleus never had less than 1-MeV excitation.[28]

(2) A second particle was selected (also a neutron) and for the maximum excitation following emission of the particle in 1, the probabilities for all possible kinetic energies of emission of the second particle were calculated, multiplied by the probability for populating the initial state in 1, and stored according to residual excitation.

(3) For the second highest residual excitation following emission of the first particle, process 2 was repeated etc., until all possible energies of the second particle had been calculated for all energies of the first particle and stored (and summed) according to residual excitation.

(4) The second particle emitted was changed to p, d, t, He³, and finally He⁴ and steps 2 and 3 were repeated. The initial energy always was taken to be equal to $\epsilon_0 V_i + 0.25$ MeV, and the distribution of residual nuclei resulting from nn, np, nd, nt, nHe³, and nHe⁴ reactions were calculated.

(5) The first particle was changed to p, then d, etc. Steps 1 to 4 were repeated, yielding distributions of residual nuclei as a function of excitation energy. The residual nuclei resulted from 36 different combinations of two particle emission from the original compound nucleus at a given initial excitation energy.

(6) The initial excitation energy was decreased by 2 MeV and the process (1)-(5) repeated, etc., until no more particle emission was possible. In some circumstances the residual nuclei still had a range of excitations where two or more different third particles could be emitted. In these cases, the pertinent spectra were used as input into a second program which calculated probabilities as in (2)-(5).

A level density expression of the form given by Eq. (4) becomes physically meaningless if $0 \leqslant E \leqslant \delta$. In these calculations we assume that neutron and proton emissions that produce residual nuclei with excitations $0 \leqslant E \leqslant \delta$ are possible and take precedence over gamma emission. A proton, however, is always required to be emitted with an energy that is greater than ϵ_c.[29]

IV. RESULTS AND DISCUSSION

The total emission probabilities were normalized to the cross section for the formation of a compound

[28] Graphical integration showed that 0.5-MeV divisions gave results correct to 99%.
[29] This restriction applies to all calculated curves (Figs. 6 to 10) and is discussed in greater detail in the next section.

nucleus by the bombardment of Ni^{58} with deuterons. This deuteron compound nucleus formation cross section has been discussed in Sec. III. The situation sometimes occurred in which neutron emission was not possible, but in which sufficient excitation energy was available to emit a proton below the effective barrier, ϵ_c. In these situations, integrations to obtain total cross sections were made with two extreme assumptions:

(I) It was assumed that gamma emission would not compete with charged particle emission below the effective barrier, i.e., $\Gamma_\gamma/\Gamma_{total}=0$, when $\epsilon < \epsilon_c$.

(II) It was assumed that charged particle emission would not compete with gamma emission below the effective barrier, i.e., $\Gamma_\gamma/\Gamma_{total}=1$, when $\epsilon < \epsilon_c$.

Calculated excitation functions are compared with experimental excitation functions in Figs. 5–10. Theoretical excitation functions calculated with assumption I go through a maximum at lower excitation energies than the experimental curves. The broken curves of Fig. 5, for example, show (d,α) and $(d,\alpha n)$ excitation functions calculated with assumption I.

The curves b and c of Figs. 6–10 calculated with assumption II about $\Gamma_\gamma/\Gamma_{total}$, are in closer agreement with experimental excitation functions. That assumption II gives closer agreement with experimental results is consistent with the extremely steep decrease in the proton inverse cross sections in the region below ϵ_c (Fig. 3). The curves marked b in Figs. 6–10 are calculated with only one independent assumption: The radius factor used to calculate the compound-nucleus formation cross section is 1.1 F (as discussed in Sec. C4). The agreement between the experimental curves a and the calculated curves b is fairly close despite the uncertainty in the values of σ_{inv}.

The optical-model total nonelastic cross sections include inelastic reactions that do not result in compound nucleus formation (as indicated in Sec. IIIB 2). A second set of inverse proton and alpha particle cross sections corresponding to smaller nuclear radii were therefore calculated. The curves marked c in Figs. 6–10 were

FIG. 7. Curve a is the experimentally determined $Ni^{58}(d,\alpha p)Fe^{55}$ excitation function. Curves b and c are statistical theory calculations for the two different sets of inverse cross-section parameters. Curve b corresponds to set (1) and curve c to set (2).

FIG. 5. The solid lines are the experimentally determined $Ni^{58}(d,\alpha)Co^{56}$ and $Ni^{58}(d,\alpha n)Co^{55}$ excitation functions. The dashed lines are statistical theory calculations corresponding to the first set of capture cross section parameters and assumption I about $\Gamma_\gamma/\Gamma_{total}$.
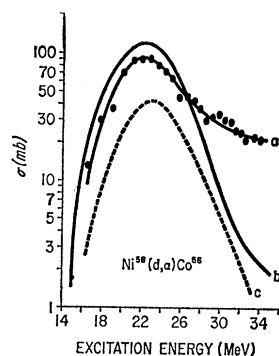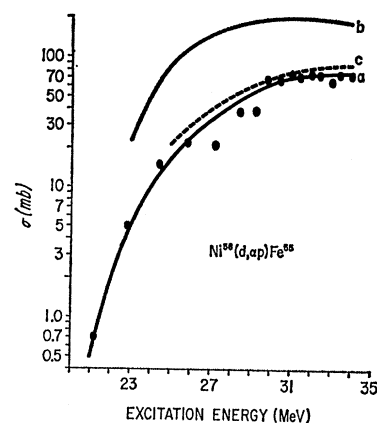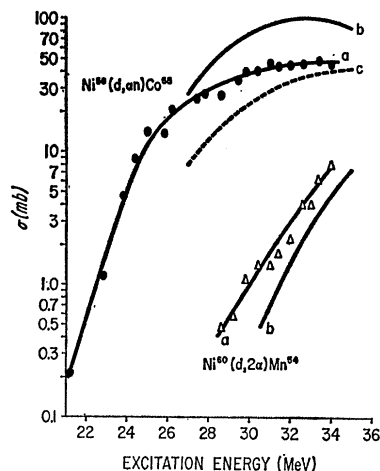

FIG. 6. Curve a is the experimentally determined $Ni^{58}(d,\alpha)$-Co^{56} excitation function. Curves b and c are statistical theory calculations for the two different sets of inverse cross-section parameters. Curve b corresponds to set (1) and curve c to set (2).

FIG. 8. Upper curve a is the experimentally determined $Ni^{58}(d,\alpha n)Co^{55}$ excitation function. Curves b and c are statistical theory calculations for the two sets of inverse cross-section parameters. Curve b corresponds to set (1) and curve c to set (2). For the $Ni^{60}(d,2\alpha)Mn^{54}$ reaction: Lower curve a is the experimental excitation function and curve b is the theoretical curve calculated with the same assumptions as curves b of the Ni^{58} reactions. The Mn^{54} produced could also be due to a $Ni^{58}(d,\alpha 2p)Mn^{54}$ reaction, as discussed in note b of Table II.

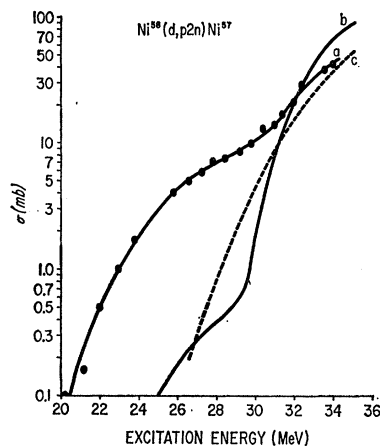FIG. 9. Curve a is the experimentally determined Ni⁵⁸-$(d,p2n)$Ni⁵⁷ excitation function. Curves b and c are statistical theory calculations for the two different sets of inverse cross-section parameters. Curve b corresponds to set (1) and curve c to set (2).
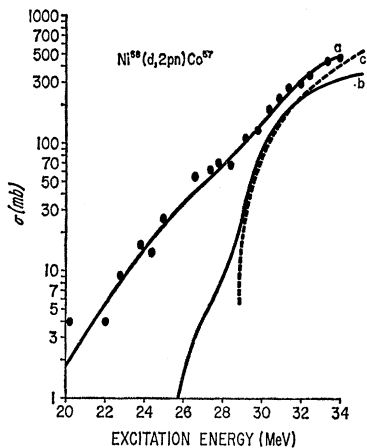

FIG. 10. Curve a is the experimentally determined Ni⁵⁸-$(d,2pn)$Co⁵⁷ excitation function. Curves b and c are statistical theory calculations for the two different sets of inverse cross-section parameters. Curve b corresponds to set (1) and curve c to set (2).

calculated with this second set of cross sections. In general, the experimental excitation functions tend to lie between curves b and c. The Ni⁶⁰$(d,2\alpha)$Mn⁵⁴ excitation function (Fig. 6, curve b) was calculated as Ni⁵⁸$(d,2\alpha)$Mn⁵².

As mentioned in Sec. I, these excitation-function measurements were partially motivated by a desire to obtain nuclear reactions which could be interpreted in terms of the compound nucleus theory and the statistical mechanics of highly excited nuclei. The interpretation of experimental nuclear data in terms of the compound nucleus theory as applied to the continuum is nearly always complicated by the presence of non-random direct interactions. The large divergence between the experimental cross sections and the theoretical calculations shown in Fig. 6 for the high-energy tail of the (d,α) excitation function may be due to (d,α) direct interactions. The magnitude of the (d,α) tail is consistent with the magnitude of the direct interaction components of Cu(d,α)Ni scattering with 24-MeV deuterons.[11] The large divergence between the experimental cross sections and the calculated compound-nucleus cross sections in the threshold regions of the $(d,p2n)$ and $(d,2pn)$ curves, (Figs. 9 and 10) can prob-

ably be accounted for by (d,H^3) and (d,He^3) pick-up reactions, respectively.[11,30] The small theoretical (d,H^3) and (d,He^3) compound-nucleus cross sections are included in the theoretical $(d,p2n)$ and $(d,2pn)$ cross-section curves and account for the inflections in the threshold region of these curves. However, the divergence between the experimental and theoretical calculations cannot be explained in terms of (d,H^3) and (d,He^3) compound nucleus reactions.

V. CONCLUSIONS

The decrease in the Ni⁵⁸(d,α)Co⁵⁶ excitation function cross sections above the thresholds of competing reactions is in qualitative agreement with a compound nucleus reaction mechanism. The statistical theory calculations based on Eq. (2) give fair agreement with experimental cross sections when (a) the value of parameter a is that determined independently from Ni⁵⁸(p,α) spectra, (b) the parameter δ is considered a pairing energy determined from experimental mass values, (c) optical-model total nonelastic cross sections are used to represent inverse reaction cross sections, (d) it is assumed that charged particle emission cannot compete with gamma emission below ϵ_c, and (e) the deuteron compound nucleus cross section is calculated with a nuclear radius constant of 1.1 F.

For reasons of simplicity and practicality, we have used the form of the compound nucleus theory based on the assumption that the distribution of angular momentum states in residual nuclei is proportional to $(2J+1)$ although both experimental and theoretical investigations indicate that a spin dependency of the form $(2J+1)\exp(-J^2/2\sigma^2)$ would have greater validity at high-excitation energies.[11,31,32] A knowledge of the distribution of nuclear states over a wide range of excitation energies is necessary in order to calculate excitation function cross sections resulting from the emission of multiple particles in cascade. A more precise statistical-theory calculation encounters the difficulty that at low excitation energies neither a level-density expression of the form $(2J+1)E^{-2}\exp\{2(aE)^{1/2}\}$ or of the form $(2J+1)E^{-2}\exp(-J^2/2\sigma^2)\exp\{2(aE)^{1/2}\}$ is an accurate description of the distribution of nuclear levels. This is especially true in the region of closed, or doubly closed shells, i.e., Ni⁵⁶.[33-36]

ACKNOWLEDGMENTS

We wish to thank R. Thakore and Dr. P. Eberlein of the University of Rochester computing center for aid in writing and debugging the statistical-theory program,

[30] J. Gonzales-Vidal and W. H. Wade, Phys. Rev. **120**, 1324 (1960).
[31] H. W. Fulbright, N. O. Lassen, and N. O. Roy Poulsen, Kgl. Danske Videnskab. Selskab, Mat. Fys. Medd. **31**, No. 10 (1959).
[32] J. Benveniste, G. Merkel, and A. Mitchell, Bull. Am. Phys. Soc. **7**, 454 (1962).
[33] C. Bloch, Phys. Rev. **93**, 1086 (1954).
[34] N. Rosenzweig, Phys. Rev. **108**, 817 (1957).
[35] A. A. Ross, Phys. Rev. **108**, 720 (1957).
[36] T. D. Newton, Can. J. Phys. **34**, 804 (1956).

and to offer our very sincere appreciation to Dr. Henry Mullish of the NYU Computing Center for the wonderful hospitality accorded to us on our visits to the AEC computing center. Our thanks for bombardments to W. B. Jones and the crew of the former University of California 60 in. cyclotron, to Leon Schwartz for the drawings, and to Dr. E. Schwarcz of Lawrence Radiation Laboratory for help in running the optical-model calculations. We are grateful to Dr. John Huizenga, Dr. Bruce Foreman, and Dr. Michel Melkanoff for many helpful discussions.

The authors wish to express gratitude to Professor A. C. Helmholz, Professor G. T. Seaborg, and Professor E. O. Wiig for their support of this work.

Alpha Decay of Cf^{246}†

A. M. FRIEDMAN AND J. MILSTED

Argonne National Laboratory, Argonne, Illinois

(Received 4 February 1963)

A sample of Cf^{246} was prepared by intensive alpha bombardment of Cm^{244}. The alpha spectrum was studied by use of silicon surface barrier detectors having a resolution of 18 keV at 6.7-MeV alpha energy. The alpha energies and intensities found for the transitions were: 6.753 MeV, 77.9±0.2%; 6.714±0.0007 MeV, 21.9±0.2%; 6.621±0.001 MeV, 0.18±0.02%; and 6.465±0.003 MeV, undetermined intensity. The energies can be fitted by the expression

$$E = 6.46I(I+1) + 0.0074I^2(I+1)^2 \text{ keV}$$

and the relative intensities by $C_0:C_2:C_4 = 1:0.42:0.080$, where the C's are the reciprocals for the hindrance factors of the various L waves.

TEN milligrams of Cm^{244} containing 2% Cm^{246} by mass were bombarded for 100 h in the Argonne 60-in. cyclotron. After the bombardment the resulting products were chemically purified and samples of the californium fraction were volatilized onto backing disks for alpha and fission counting. For the first two weeks essentially all the californium activity was due to Cf^{246}. The singles alpha spectrum was obtained by use of a silicon surface barrier detector and a 400-channel pulse-height analyzer. The fissions were counted in a small fast ion chamber using pulse-height discrimination to sort out the alpha pulses. The alpha to fission ratio so found gave a fission half-life of 1340±160 yr in reasonable agreement with the value of 2100 yr of Hulet, Thompson, and Ghiorso[1] for an alpha half-life of 36 h.

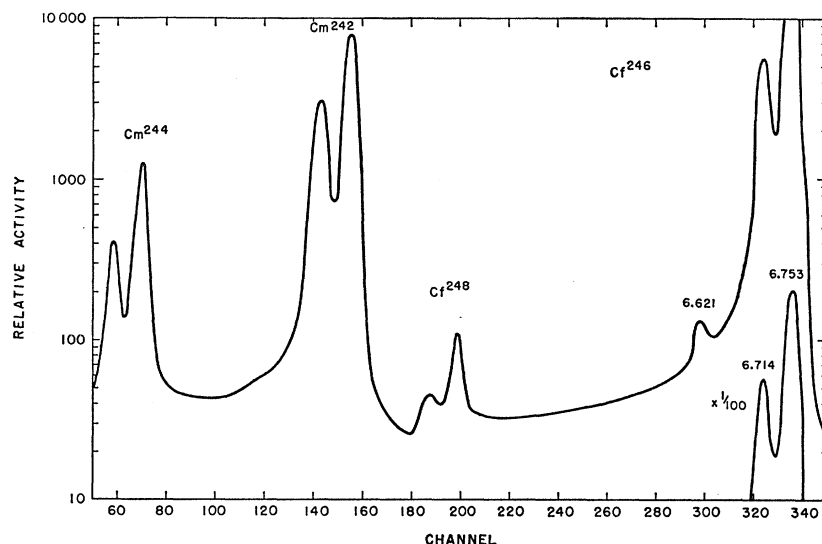The alpha singles spectrum is shown in Fig. 1. The

FIG. 1. Alpha singles spectrum of Cf^{246}.

[1] E. K. Hulet, S. G. Thompson, and A. Ghiorso, Phys. Rev. **89**, 878 (1953).